

10/19/92 8:50

Conf. 9208107-37
SLAC-PUB-5900

HIGH-GRADIENT STUDIES ON 11.4 GHz COPPER ACCELERATOR STRUCTURES SLAC-PUB-5900

J.W. Wang, R.A. Curry, H. Deruyter, H.A. Hoag, R.F. Koontz, G.A. Loew,

A. Menegat, R.H. Miller, R.D. Ruth, A. E. Vlieks, C. Yoneda

DE93 001818

Stanford Linear Accelerator Center

Stanford, California 94309, USA

Abstract

This paper is a progress report on studies carried out at SLAC to assess the high-gradient behavior of 11.4 GHz copper accelerator structures for future linear colliders. The structures which have been examined in the last year are a 7-cavity standing-wave (SW) section and a 30-cavity traveling-wave (TW) section. Both structures are of the constant-impedance uniform-aperture type with a $2\pi/3$ phase shift per cavity. The results presented here include new information on RF breakdown, field emission, RF processing and dark current. The captured dark current depends on the rise time of the RF pulse.

Introduction and Experimental Set-up

Work on the high-gradient behavior of accelerator structures for future linear colliders started at SLAC in 1984 with experiments at S-Band (2.856 GHz). The most recent report summarizing the SLAC results as of September 1990 can be found in reference [1]. The work presented here has been done since that time and applies only to X-Band (11.42 GHz). It has been made possible by the development at SLAC of X-Band klystrons and the so-called Binary-Pulse Compression (BPC) system [2]. The maximum peak power from a klystron was 30 MW with a pulse width of 800 ns at 60 pps. When combined with the BPC, it produced up to about 80 MW peak power with a 60 nsec pulse width. Experience with earlier breakdown and field emission experiments was used to plan the tests described below.

The first test was done on a 7-cavity standing-wave (resonant) section, very much like an earlier 7-cavity standing-wave S-Band section [1], since the peak power available at first from the X-Band klystron was too low to obtain the breakdown limit expected at this frequency in a non-resonant structure.

With increased power and the use of the BPC, the second test was done on a 30-cavity traveling-wave structure with a symmetrically fed input coupler cavity. Both structures were of the constant-impedance uniform-aperture type. Aside from the power source, it was necessary to provide the proper shielded environment to carry out the high radiation tests. A bunker adjacent to the klystron test-stands was built and is shown in Fig. 1. The rectangular waveguide bringing the power from the klystron and BPC can be seen on the right with several vacuum pumps, and the dual input of the traveling-wave section can be seen on the left, also surrounded by vacuum pumps. The layouts of the respective set-ups are shown in Fig. 2.

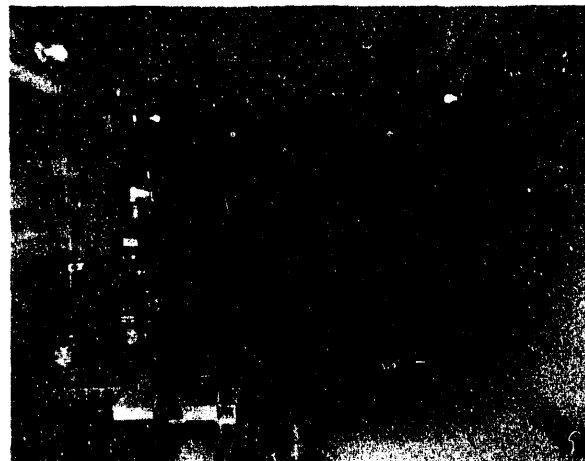


Fig. 1 Experimental set-up inside bunker for high power tests of the 30-cavity TW section. The SW section set-up was very similar.

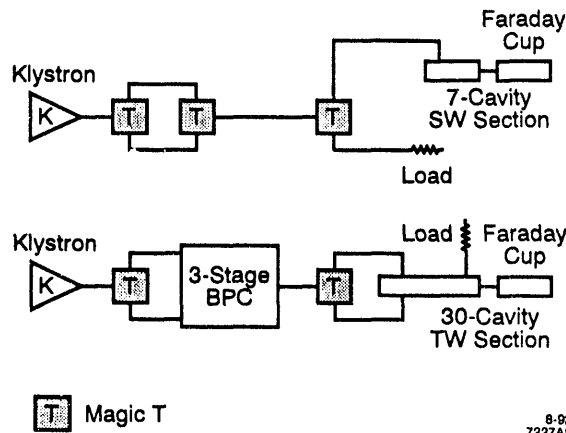


Fig. 2. RF system layouts for high power tests of the 7-cavity SW and 30-cavity TW sections .

Note that the SW test did not require the BPC but used a Magic Tee to partially decouple the klystron from the reflections from the section. The straight-ahead Faraday cup was constructed from a modified commercial (MDC) feedthrough combined with a tantalum cylinder and a graphite cap. A coaxial shield was added to suppress electrical noise. Momentum analysis of the captured field-emitted current was not yet available. A Residual Gas Analyzer (RGA) was attached to the vacuum system.

Experimental Results

The characteristics of the two X-Band sections and the experimental results are shown in Table 1. The S-Band results obtained earlier are shown in the first column for reference and

* Work supported by Department of Energy contract DE-AC03-76SF00515.

Presented at the Linac '92 Conference, Ottawa, Canada, August 24-28, 1992.

MASTER

comparison. Note that the maximum surface field on the disk, E_s , reached 500 MV/m in the SW section (as compared to 310 MV/m in the corresponding S-Band section) but could not be measured in the TW section because of insufficient power. The breakdown limit did not vary much when the RF pulse was shortened from 800 to 200 ns.

TABLE 1

| | S-Band 7-Cavity (SW) | X-Band 7-Cavity (SW) | X-Band 30-Cavity (TW) |
|---------------------------------|----------------------------|----------------------------|-----------------------------|
| Frequency f (MHz) | 2856 | 11424 | 11424 |
| Iris diameter, 2a (cm) | 1.99 | 0.75 | 0.75 |
| Cavity diameter, 2b (cm) | 8.19 | 2.12 | 2.12 |
| Total length (cm) | 24.5 | 6.13 | 26.25 |
| Shunt impedance ($M\Omega/m$) | 62.6/2 | 98/2 | 98 |
| Factor of merit, Q | 13800 | 6960 | 6960 |
| Input coupler type | Single | Single | Double |
| Filling time (ns) | 770 | 80 | 26.5 |
| RF pulse length (ns) | 2500 | 800 | 60 |
| Peak input power (MW) | 47* | 14* | 75† |
| Max. surf. E_s (MV/m) | 310* | 500* | 194† |
| Max. av. E_{acc} (MV/m) | 80* | 110* | 85† |
| Field enhancement β | 60 | 50 | — |
| E_s/E_{acc} | 3.88 | 4.55 | 2.28 |

* Limited by RF breakdown

† Limited by klystron output power

Fig. 3 shows typical pulse shapes for the 7-cavity SW section tests. The dark current or field-emitted current measured by the Faraday cup is seen to reach its asymptotic peak after about 160 nsec or two filling times. Fig. 4 gives this peak current as a function of maximum surface field which in the resonant case occurs only in the 3rd and 6th cavity from the coupler. From the theory of linear accelerator injectors, it can be shown that an electron at rest on axis will be captured by a velocity-of-light traveling-wave if the peak accelerating field in MV/m reaches $1.6/\lambda(m)$, i.e., 61 MV/m at 11.42 GHz. In this figure, this

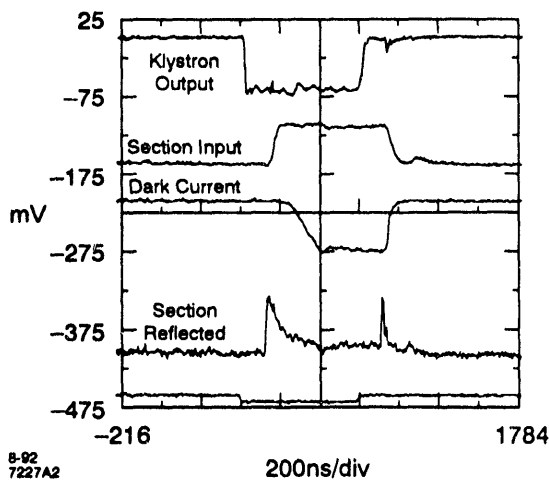


Fig. 3. Pulse shapes of klystron output, section input, reflected power, and dark current for 7-cavity SW section.

corresponds to about 280 MV/m surface field. Of course, the 7-cavity section is so short that even some of the electrons that are not captured are likely to reach the Faraday cup. At the higher field levels, a momentum analysis would probably show a double-peaked curve corresponding to the contributions from the two high-field cavities. When the surface field reached 500 MV/m, the current was 120 mA and the radiation dosage around the section was ~ 700 R/hr. For $E_{acc} \sim 50$ MV/m (just below capture) the peak current was about 0.5 mA. Fig. 5 shows a typical Fowler-Nordheim plot from which the field enhancement factor β can be obtained by using the standard formula given in Reference 1. The value of β depends on which portion of the curve is taken but is about 50 if one takes the portion above 280 MV/m where true capture occurs.

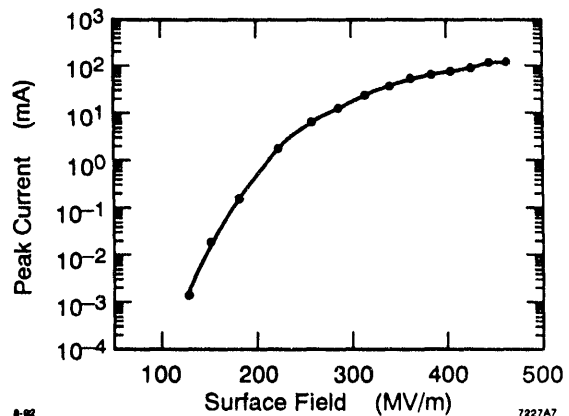


Fig. 4. Peak dark current measured by Faraday cup as a function of maximum surface field on disks of 7-cavity SW section.

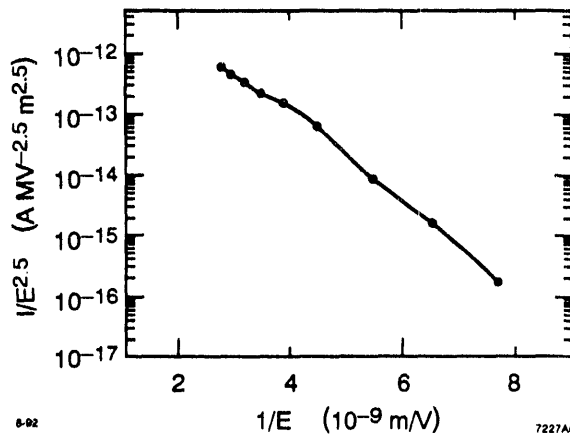


Fig. 5. Fowler-Nordheim plot for 7-cavity section tests.

Fig. 6 shows the effect of RF processing on dark current in the TW section during two distinct periods separated by several weeks of downtime during which the klystron was repaired. Both processing periods lasted 40 hours. The maximum field of 85 MV/m (limited by klystron output) was reached after a total of 80 hours at the end of which the dark current as a function of E_{acc} fell along the curve of June 24, 1992. The peak current was about 2 mA at 85 MV/m vs. 10 μ A at 50 MV/m. These numbers are fairly consistent with the SW ones. Assuming that

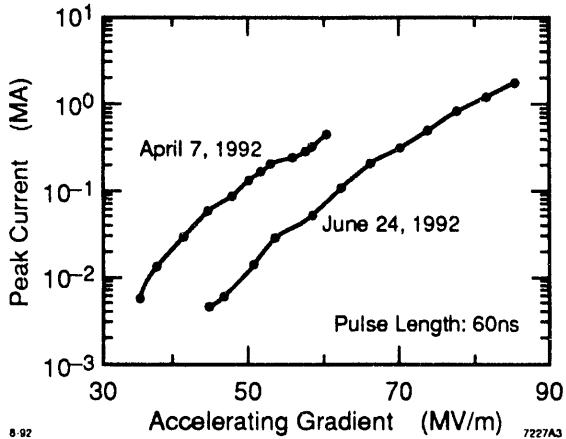


Fig. 6. Peak dark current measured by Faraday cup as a function of average accelerating field for two stages of RF processing.

one is close enough to the capture threshold at 50 MV/m to catch most of the electrons, this would indicate that each of the 30 cavities contributes $0.33 \mu\text{A}$ or about 10^5 e^- in 60 nsec. Fig. 7 shows the RF pulse shapes and dark current for three different pulse rise times. This is probably the most revealing piece of information in this paper. It shows that for a steep input rise time of about 10 ns (Fig. 7a), which probably causes an upward frequency shift of several tens of megahertz (and a slight overshoot in amplitude), the capture is significantly increased. When the frequency shift subsides after about a filling time (26.5 ns), the dark current subsides accordingly. The effect becomes less pronounced as the rise time increases to about 15 nsec (Fig. 7b) and disappears completely for a rise time of about 20 nsec (Fig. 7c). This effect can be explained by the fact that the higher frequency leads to a lower phase velocity which causes more electrons to be captured. This hypothesis was verified by changing the RF drive frequency for the entire pulse (Fig. 8) and observing the increase in dark current at a fixed value of average E_{acc} (77 MV/m). As this paper is being

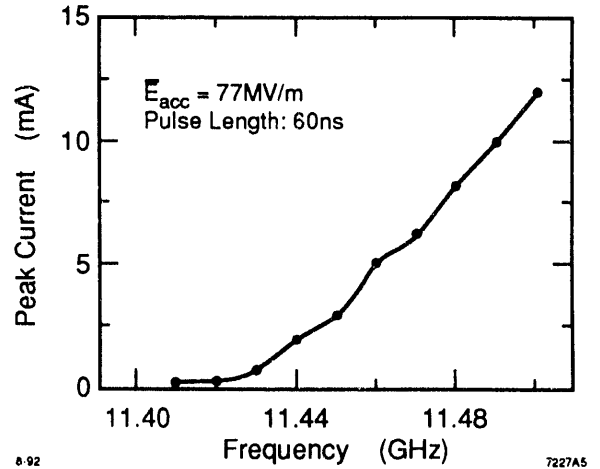


Fig. 8. Peak dark current as a function of RF frequency.

written, the BPC is being equipped with two klystrons at the input which will boost the peak power to about 200 MW. The tests on the TW section will then be resumed to obtain fields above 100 MV/m. Later in the year, new 75 cm and 180-cm-long sections will become available for more definitive tests.

References

- [1] G. A. Loew and J. W. Wang, "Progress Report on High-Gradient RF Studies in Copper Accelerator Structures", presented at the XIVth Int. Symp. on Discharges and Electrical Insulation in Vacuum, Santa Fe, New Mexico, September 16-20, 1990. Available as SLAC-PUB-5320.
- [2] Z. D. Farkas, "Binary Peak Power Multiplier and its Application to Linear Accelerator Design", IEEE Trans. MTT-34, 1036, 1986, SLAC-PUB-3694, May 1985.

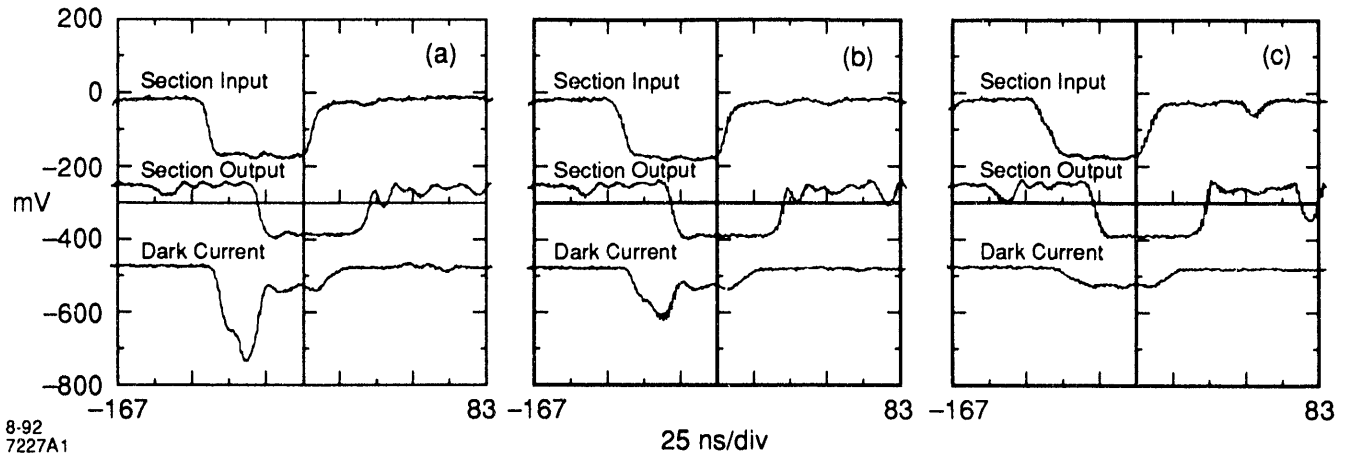


Fig. 7. Pulse shapes of section input, output and dark current for three different rise times of the RF pulse for 30-cavity TW section tests.

END

**DATE
FILMED**

11/10/92

